



Analytical Solution in Curvilinear Coordinates for the Trajectory of a Projectile Subject to Aerodynamic Drag

by Steven B. Segletes and William P. Walters

ARL-TR-5822

December 2011

NOTICES

Disclaimers

The findings in this report are not to be construed as an official Department of the Army position unless so designated by other authorized documents.

Citation of manufacturer's or trade names does not constitute an official endorsement or approval of the use thereof.

Destroy this report when it is no longer needed. Do not return it to the originator.

Army Research Laboratory

Aberdeen Proving Ground, MD 21005-5066

ARL-TR-5822**December 2011**

Analytical Solution in Curvilinear Coordinates for the Trajectory of a Projectile Subject to Aerodynamic Drag

Steven B. Segletes and William P. Walters

Weapons and Materials Research Directorate, ARL

REPORT DOCUMENTATION PAGE				Form Approved OMB No. 0704-0188	
<p>Public reporting burden for this collection of information is estimated to average 1 hour per response, including the time for reviewing instructions, searching existing data sources, gathering and maintaining the data needed, and completing and reviewing the collection information. Send comments regarding this burden estimate or any other aspect of this collection of information, including suggestions for reducing the burden, to Department of Defense, Washington Headquarters Services, Directorate for Information Operations and Reports (0704-0188), 1215 Jefferson Davis Highway, Suite 1204, Arlington, VA 22202-4302. Respondents should be aware that notwithstanding any other provision of law, no person shall be subject to any penalty for failing to comply with a collection of information if it does not display a currently valid OMB control number.</p> <p>PLEASE DO NOT RETURN YOUR FORM TO THE ABOVE ADDRESS.</p>					
1. REPORT DATE (DD-MM-YYYY) December 2011		2. REPORT TYPE Final		3. DATES COVERED (From - To) June 2011 - October 2011	
4. TITLE AND SUBTITLE Analytical Solution in Curvilinear Coordinates for the Trajectory of a Projectile Subject to Aerodynamic Drag				5a. CONTRACT NUMBER	
				5b. GRANT NUMBER	
				5c. PROGRAM ELEMENT NUMBER	
6. AUTHOR(S) Steven B. Segletes William P. Walters				5d. PROJECT NUMBER AH80	
				5e. TASK NUMBER	
				5f. WORK UNIT NUMBER	
7. PERFORMING ORGANIZATION NAME(S) AND ADDRESS(ES) U.S. Army Research Laboratory ATTN: RDRL-WMP-C Aberdeen Proving Ground, MD 21005-5066				8. PERFORMING ORGANIZATION REPORT NUMBER ARL-TR-5822	
9. SPONSORING/MONITORING AGENCY NAME(S) AND ADDRESS(ES)				10. SPONSOR/MONITOR'S ACRONYM(S)	
				11. SPONSOR/MONITOR'S REPORT NUMBER(S)	
12. DISTRIBUTION/AVAILABILITY STATEMENT Approved for public release; distribution is unlimited.					
13. SUPPLEMENTARY NOTES					
14. ABSTRACT An analytical study was conducted to determine the general trajectory of a projectile subject to aerodynamic drag in a gravitational field. A solution was obtained to the governing equations using curvilinear coordinates. The general solution analytically provides the pathlength of the projectile in terms of the current trajectory angle. Noticeably absent from the solution, however, are several desirable quantities. For instance, there is no ability to analytically express the trajectory of the projectile in Cartesian (x, y) coordinates; analytically express the time of the event in terms of an independent variable; and analytically invert the solution to express the trajectory angle in terms of, for example, the pathlength. Nonetheless, the solution does provide the velocities (x, y , and pathlength) in terms of the current trajectory angle, as well as the time rate of change of the trajectory angle in terms of the current trajectory angle. For applications where a Cartesian solution and/or time history is required, the current solution permits an expedited numerical integration as compared to a general-purpose integration of the governing equations, as well as an analytical approximation valid for moderate angles of attack. Finally, an interesting analytical result was developed that shows that the launch angle required to maximize the pathlength to the apogee is always 56.5° , regardless of drag coefficient, initial projectile velocity, or even gravitational constant.					
15. SUBJECT TERMS aerodynamic drag, range safety, particle trajectory, analytical solution					
16. SECURITY CLASSIFICATION OF:			17. LIMITATION OF ABSTRACT UU	18. NUMBER OF PAGES 38	19a. NAME OF RESPONSIBLE PERSON Steven B. Segletes
a. REPORT Unclassified	b. ABSTRACT Unclassified	c. THIS PAGE Unclassified			19b. TELEPHONE NUMBER (Include area code) 410-278-6010

Contents

List of Figures	v
List of Tables	vi
Acknowledgments	vii
1. Introduction	1
2. Flight Retardation Equations (Cartesian Coordinates)	2
3. Flight Retardation Equations (Curvilinear Coordinates)	3
4. Relating \dot{s} and $\dot{\alpha}$ Without Curvilinear Coordinates	4
5. Second-order Governing Relation in One Variable	5
6. Integrating the Second-order Governing Equation	6
7. Ancillary Velocity Variables	7
8. Integrating for the Trajectory Pathlength	8
9. Known and Unknown	8
10. Expedited Numerical Integration for Cartesian Trajectory	10
11. Special Case Solutions and Approximations	14

11.1	Approximate Cartesian Solution for Moderate Angle-of-attack Trajectories	14
11.2	Maximum Pathlength from Launch to Apogee	18
11.3	Terminal Trajectory	19
12.	Conclusions	21
13.	References	22
	Distribution List	23

List of Figures

Figure 1. Velocity diagram.	3
Figure 2. Trajectory (y) and velocity (ds/dt) for 50 mm-long copper ($\rho_p = 8900 \text{ kg/m}^3$) projectile with $C_d = 1.0$ ($B = 0.00145/\text{m}$) launched at 2000 m/s at an angle of $\alpha_0 = 25^\circ$ from an initial altitude of $H = 1 \text{ m}$	12
Figure 3. Pathlength (s), velocity (ds/dt), and flight time (t) as a function of trajectory angle (α).	13
Figure 4. $\dot{\alpha}$ and $d\alpha/ds$ as a function of trajectory angle (α).	13
Figure 5. A comparison of $\tan \alpha \sec \alpha + \ln(\tan \alpha + \sec \alpha)$ to the approximation given by $2 \tan \alpha$	15
Figure 6. A comparison of numerically integrated (black) and approximated (red) trajectories for initial trajectory angles below 20°	17
Figure 7. A comparison of numerically integrated (black) and approximated (red) trajectories for initial trajectory angles between 25° and 40°	17
Figure 8. Estimated terminal trajectories from three starting points on the actual trajectory, corresponding to α_t equal to 0° , -30° , and -60° , respectively.	20

List of Tables

Table 1. FORTRAN code listing. 11

Acknowledgments

We would like to thank Mr. Cyril Williams for his thoughtful and diligent review of both this report and its predecessor, ARL-TR-5612.

INTENTIONALLY LEFT BLANK.

1. Introduction

The classical trajectory problem in a uniform gravitational field is well known, if there are no drag forces on the projectile. The trajectory traces out a parabolic path in the atmosphere over time, while the horizontal component of velocity remains undiminished. In the real world, however, the projectile is subject to drag forces, which, at high Reynolds number, are estimated to be proportional to the square of the velocity (*i.e.*, aerodynamic drag). This drag force complicates the solution of the trajectory.

Prior studies attempting to analytically address the issue have been limited to a variety of approximate methods, *e.g.*, (1). Alternately, others (2) have modified the assumption of aerodynamic drag in favor of a (less physically based) constant-deceleration approximation. Along similar lines, some (3) redefine the drag as viscous (*i.e.*, proportional to velocity V), rather than aerodynamic (proportional to V^2). Still others (4) develop separate equations for pure-vertical and pure-horizontal flight, under the influence of aerodynamic drag, and then assume (by way of approximation) that they can be respectively applied to the vertical and horizontal components of an arbitrary trajectory. With the advent of a pervasive computing environment, numerical approaches can be adopted to calculate trajectory solutions. However, numerical solutions, which apply only to a particular set of initial conditions, fail to provide the functional understanding of trajectory behavior afforded by an analytical solution.

A prior analytical study was conducted (5) to determine the distance a hypervelocity projectile would travel in air. In that study, special cases of the more general problem were analytically solved, such as vertical launch and/or small-angle (*i.e.*, near horizontal) trajectory. In the current effort, the more general case of arbitrary launch angle and large changes in the trajectory are considered. The projectile is ballistic, by which we mean capable of neither propulsion nor lift. The model is based on Newton's 2nd Law and the sole forces acting on the projectile are drag and gravity. Erosion, ablation, and strength of the projectile are not considered. This study is useful for experimental-range safety considerations, as well as fragment lethality and fragment recovery.

The problems of range safety and danger areas have been examined in the past (6), with aerodynamic drag being applied to various ballistic projectiles. However, such prior studies have not put forth analytical relations, such as those pursued in the current work.

2. Flight Retardation Equations (Cartesian Coordinates)

Consider a projectile of mass m launched at an initial velocity $V = V_0$, at an angle α_0 with respect to the horizon, subject to the initial (time $t = 0$) conditions that the horizontal position $x = 0$, and the vertical position y takes on a value of H , representing the height above ground of the launch.

The velocity components at any given moment are given as

$$v_x = \dot{x} = V \cos \alpha \quad (1)$$

and

$$v_y = \dot{y} = V \sin \alpha \quad (2)$$

where α is the time-dependent trajectory angle with respect to the horizon, and the overdot denotes time differentiation. The aerodynamic drag force on the projectile is $\rho AC_d V^2/2$, where ρ is the density of air at sea level (1.293 kg/m^3), g is the acceleration due to gravity (9.806 m/s^2), C_d is the drag coefficient, and A is the effective cross-sectional area (m^2). The governing equations, accounting for the effects of aerodynamic drag and gravity and neglecting ablation, according to Newton's 2nd Law, are:

$$m\ddot{x} = -\frac{\rho AC_d V^2}{2} \cos \alpha = -\frac{\rho AC_d}{2} \dot{x} \sqrt{\dot{x}^2 + \dot{y}^2} \quad (3)$$

and

$$m\ddot{y} = -\frac{\rho AC_d V^2}{2} \sin \alpha - mg = -\frac{\rho AC_d}{2} \dot{y} \sqrt{\dot{x}^2 + \dot{y}^2} - mg \quad (4)$$

By lumping the term, $B = \rho AC_d/2m$, we may restate the governing set of equations (in Cartesian coordinates) as

$$\ddot{x} = -B\dot{x}\sqrt{\dot{x}^2 + \dot{y}^2} \quad (5)$$

$$\ddot{y} = -B\dot{y}\sqrt{\dot{x}^2 + \dot{y}^2} - g \quad (6)$$

The grouping within B , given by m/A , represents the areal density along the flight axis of the projectile, and may be alternately expressed as $\rho_p L_p$, where ρ_p is the projectile density and L_p is the characteristic length of the projectile. Thus, an alternative expression for B is given by $B = \rho C_d/2\rho_p L_p$. Note, that in reference 4 equation 5 is solved assuming $\dot{y} = 0$, and equation 6 is solved assuming $\dot{x} = 0$, resulting in greatly simplified, but approximate, solutions.

3. Flight Retardation Equations (Curvilinear Coordinates)

Define direction s as the coordinate along the flight trajectory, and n as the direction normal to the current trajectory. Because the curvilinear coordinate system follows the trajectory, the coordinate n will always be identically zero, even as there are forces bending the coordinate system in the n direction. For example, there is a component of the gravitational force in both the s and n directions. Additionally, there is aerodynamic drag along the axial s direction. The governing equations, in curvilinear coordinates, are therefore

$$\ddot{s} = -g \sin \alpha - B\dot{s}^2 \quad (7)$$

$$\ddot{n} = g \cos \alpha \quad (8)$$

The tendency of the trajectory (and the coordinate system) to bend by way of equation 8 may be related to changes in the trajectory angle α . From a velocity diagram, figure 1,

$$-\tan d\alpha = \frac{v_n}{v_s} = \frac{\ddot{n} dt}{\dot{s}} \approx -d\alpha \quad (9)$$

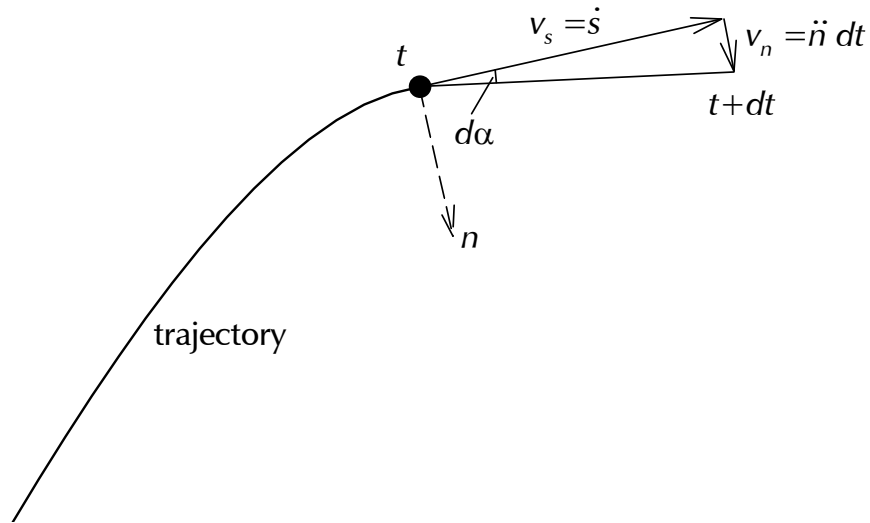


Figure 1. Velocity diagram.

Employ $\dot{\alpha} = d\alpha/dt$ and rearrange:

$$-\dot{\alpha}\dot{s} = \ddot{n} \quad . \quad (10)$$

Significantly, this equation relates lateral forces on the projectile to the speed and changes in the trajectory of the projectile. Substitute equation 8 to eliminate \ddot{n} :

$$\dot{\alpha}\dot{s} = -g \cos \alpha \quad . \quad (11)$$

Equation 11 essentially replaces the \ddot{n} relation of equation 8 as the second governing equation, in addition to equation 7. We thus have two curvilinear governing equations, in terms of s and α and their derivatives.

4. Relating \dot{s} and $\dot{\alpha}$ Without Curvilinear Coordinates

Equation 11 can be alternately derived without the use of curvilinear coordinates, as follows.

Multiply equation 6 by \dot{x} :

$$\dot{x}(\ddot{y} + g) = -B\dot{x}\dot{y}\sqrt{\dot{x}^2 + \dot{y}^2} \quad (12)$$

and equation 5 by \dot{y} :

$$\dot{y}\ddot{x} = -B\dot{x}\dot{y}\sqrt{\dot{x}^2 + \dot{y}^2} \quad . \quad (13)$$

Subtract equation 13 from equation 12:

$$\dot{x}\ddot{y} - \dot{y}\ddot{x} + g\dot{x} = 0 \quad . \quad (14)$$

Rearrange:

$$\frac{\dot{x}\ddot{y} - \dot{y}\ddot{x}}{\dot{x}^2} = -\frac{g}{\dot{x}} \quad . \quad (15)$$

Set this result aside for a moment.

The trajectory angle α is defined as

$$\tan \alpha = \frac{\dot{y}}{\dot{x}} \quad . \quad (16)$$

Differentiate with respect to time:

$$\dot{\alpha} \sec^2 \alpha = \frac{\dot{x}\ddot{y} - \dot{y}\ddot{x}}{\dot{x}^2} \quad . \quad (17)$$

One can use the result of equation 15 to eliminate the right-hand side of equation 17:

$$\dot{\alpha} \sec^2 \alpha = -\frac{g}{\dot{x}} = -\frac{g \sec \alpha}{\dot{s}} \quad , \quad (18)$$

where the geometric pathlength relation $ds/dx = \sec \alpha$ has been used. This result becomes

$$\dot{s} = -\frac{g \cos \alpha}{\dot{\alpha}} \quad , \quad (19)$$

which is identical to the result of equation 11.

5. Second-order Governing Relation in One Variable

Take equation 19 and differentiate with respect to time:

$$\ddot{s} = g \sin \alpha + \frac{g \cos \alpha \ddot{\alpha}}{\dot{\alpha}^2} \quad . \quad (20)$$

Equate this with equation 7 to eliminate \ddot{s} :

$$-g \sin \alpha - B \dot{s}^2 = g \sin \alpha + \frac{g \cos \alpha \ddot{\alpha}}{\dot{\alpha}^2} \quad . \quad (21)$$

Employ equation 19 to eliminate \dot{s} by substitution, which leaves the equation wholly in terms of trajectory angle α and its derivatives:

$$\ddot{\alpha} + 2 \tan \alpha \dot{\alpha}^2 + Bg \cos \alpha = 0 \quad . \quad (22)$$

This second-order governing relation can also be rewritten as

$$\frac{d^2}{dt^2}(\tan \alpha) + Bg \sec \alpha = 0 \quad . \quad (23)$$

We see that, when there is no drag (*i.e.*, when $B = 0$), equation 23 yields a solution in which $\tan \alpha$ is linear in time. This corresponds to the classical parabolic solution in which \dot{x} is constant and \dot{y} is linear in time (since $\tan \alpha = \dot{y}/\dot{x}$).

6. Integrating the Second-order Governing Equation

For convenience, assign the substitution $w = \tan \alpha$. Then, the first term of equation 23 is merely \ddot{w} , which can alternately be expressed as $\dot{w} dw/dw$. In that case, equation 23 may be reexpressed as

$$\dot{w} dw = -Bg \sec \alpha dw \quad . \quad (24)$$

However, knowing the definition of w , it follows that

$$dw = \sec^2 \alpha d\alpha \quad , \quad (25)$$

leading to

$$\dot{w} dw = -Bg \sec^3 \alpha d\alpha \quad . \quad (26)$$

Being separated, this equation may be solved as

$$\dot{w}^2 = Bg [C - \tan \alpha \sec \alpha - \ln(\tan \alpha + \sec \alpha)] \quad , \quad (27)$$

where C is an integration constant. We choose to treat the large bracketed term on the right-hand side as an intermediate variable, call it u :

$$u(\alpha) = C - \tan \alpha \sec \alpha - \ln(\tan \alpha + \sec \alpha) \quad , \quad (28)$$

such that $\dot{w} = d/dt(\tan \alpha) = -\sqrt{Bg}\sqrt{u}$. The minus sign of the square root has been taken, as we know that $\tan \alpha$ must be decreasing throughout the trajectory. We further employ the chain rule to express \dot{w} as $\dot{\alpha} dw/d\alpha = \dot{\alpha} \sec^2 \alpha$. Thus, we can present equation 27 as

$$\dot{\alpha} = -\sqrt{Bg} \cdot \frac{\sqrt{u}}{\sec^2 \alpha} \quad . \quad (29)$$

Since u is a function of α alone, we note that equation 29 presents the time rate of change of the trajectory angle ($\dot{\alpha}$) in terms of the trajectory angle itself (α).

We may solve for the integration constant C from the launch conditions. Equation 11 tells us that, at launch,

$$\dot{\alpha}_0 = -\frac{g \cos \alpha_0}{V_0} \quad . \quad (30)$$

This may be employed in equation 29, at the $t = 0$ condition, to obtain $u(\alpha_0)$ and thus C as

$$C = \frac{g \sec^2 \alpha_0}{BV_0^2} + \tan \alpha_0 \sec \alpha_0 + \ln(\tan \alpha_0 + \sec \alpha_0) \quad . \quad (31)$$

It may be shown that $u > 0$ everywhere, as is required of equation 29. First, we note that

$$u(\alpha_0) = u_0 = \frac{g \sec^2 \alpha_0}{BV_0^2} \quad , \quad (32)$$

which is positive. Then, we determine that

$$\frac{du}{d\alpha} = -2 \sec^3 \alpha \quad , \quad (33)$$

which is everywhere negative. But since $d\alpha$ is negative along the trajectory, it implies that du is positive, and that the initially positive value $u = u_0$ will amplify along the trajectory.

7. Ancillary Velocity Variables

From the initial integration, resulting in equation 29 expressing $\dot{\alpha}$ as a function of α , a number of velocity variables may be immediately established. First, from equation 11, the projectile speed may be expressed in terms of α as

$$\dot{s} = \sqrt{\frac{g}{B}} \cdot \frac{\sec \alpha}{\sqrt{u}} \quad . \quad (34)$$

The Cartesian velocities are also accessible knowing, along the trajectory, that $dx = ds \cos \alpha$ and $dy = ds \sin \alpha$. It immediately follows that

$$\dot{x} = \sqrt{\frac{g}{B}} \cdot \frac{1}{\sqrt{u}} \quad (35)$$

and

$$\dot{y} = \sqrt{\frac{g}{B}} \cdot \frac{\tan \alpha}{\sqrt{u}} \quad . \quad (36)$$

For completeness sake, we present the time rate of change of the intermediate variable u , given as

$$\dot{u} = \dot{\alpha} \frac{du}{d\alpha} = 2\sqrt{Bg} \cdot \sqrt{u} \sec \alpha \quad . \quad (37)$$

At this stage, the specification of an intermediate angle (α) along the trajectory of the projectile flight is sufficient to yield the associated horizontal and vertical velocities, as well as the projectile

speed along the trajectory. Further, the time rate of change of trajectory angle is determined, as well, by equation 29.

The one unfortunate result is that, since equation 28 cannot be algebraically inverted to yield $\alpha(u)$, one is not able to determine (in closed form) the associated trajectory angle by first specifying a velocity along the trajectory.

8. Integrating for the Trajectory Pathlength

According to the chain rule, one may express ds/du as the ratio of \dot{s} and \dot{u} :

$$\frac{ds}{du} = \frac{\dot{s}}{\dot{u}} = \frac{1}{2Bu} \quad . \quad (38)$$

Separating the variables gives

$$ds = \frac{du}{2Bu} \quad . \quad (39)$$

Straightforward integration gives

$$s = \frac{\ln(u/u_0)}{2B} \quad , \quad (40)$$

where u_0 has been previously defined in equation 32. Equation 40 provides the pathlength s along the trajectory, as a function of u and, by inference, as a function of the trajectory angle α .

The analytical determination of s allows other useful relations to be algebraically constructed, for example,

$$\frac{\dot{x}}{\dot{x}_0} = e^{-Bs} \quad . \quad (41)$$

9. Known and Unknown

We have demonstrated a solution to the general trajectory problem of a ballistic projectile subject to aerodynamic drag in a gravitational field. The problem was cast in curvilinear coordinates in order to obtain the analytical solution. As a result of the two integrations of the second-order governing equation, we were able to obtain the trajectory pathlength s as a function of the trajectory angle α .

Also obtained were the Cartesian and pathlength velocity components (\dot{x} , \dot{y} , and \dot{s} , respectively) as well as the time rate of change of trajectory angle ($\dot{\alpha}$), all of which are expressed in terms of the current trajectory angle α .

Unfortunately, there are also quantities, which would be *very* useful to know, for which the current solution does *not* provide. The intermediate variable $u(\alpha)$, essential to the problem solution, may not be analytically inverted for $\alpha(u)$, even though an excellent approximation to the inversion exists* in

$$\alpha(u) \approx \pm \arctan \sqrt{\frac{-1 + \sqrt{1 + 0.3(C - u)^2}}{0.6}} \quad , \quad (42)$$

which is within 0.37% of the exact solution over the full domain. The negative result is used when $(C - u)$ is negative. However, when dealing with *exact* results, the independent variable of the problem must remain α , such that α *cannot* be analytically determined as a function of any other variable, such as pathlength s .

Secondly, while velocity components were obtained, to include Cartesian velocity components \dot{x} and \dot{y} , respectively, these are not analytically integrable using the current approach. Thus, the solution does *not* provide the Cartesian coordinates of the trajectory (x and y), as an analytical function of any of the variables in the problem. However, for the special case where the trajectory angle remains flat throughout ($\alpha \approx 0$), the horizontal position component x is adequately described by the trajectory pathlength s . Also, integrated as well as approximate analytical solutions in Cartesian coordinates are offered later in this report.

Finally, the integration of $\dot{\alpha}$ over time could not be analytically achieved. Thus, while many variables are known in terms of the trajectory parameters, the time required to reach various points on the trajectory is *not* analytically known from the current approach, even though equation 29 may be separated, with the time being precisely expressed in terms of α as

$$t = -\frac{1}{\sqrt{Bg}} \int_{\alpha_0}^{\alpha} \frac{\sec^2 \alpha}{\sqrt{u}} d\alpha \quad . \quad (43)$$

However, for the special case where the trajectory angle remains flat ($\alpha \approx 0$), one may transform time to a new variable τ , defined by the transform $d\tau/dt = \sec \alpha$, such that $\tau = 0$ when $t = 0$. The variable τ may be explicitly solved and, for this special case where $\alpha \approx 0$, one finds $t \approx \tau$ and gets

$$t_{\alpha \approx 0} \approx \tau = \frac{\sqrt{u} - \sqrt{u_0}}{\sqrt{Bg}} \quad . \quad (44)$$

*Equation 42 was developed by determining that $(C - u) = \tan \alpha \sec \alpha + \ln(\tan \alpha + \sec \alpha)$ was extremely well approximated by $(C - u) \approx 2 \tan \alpha (\sqrt{1 + 0.3 \tan^2 \alpha})$. This approximation was inverted to yield equation 42.

10. Expedited Numerical Integration for Cartesian Trajectory

Because the trajectory s is known in terms of α , an expedited numerical integration may be set up that provides the time history of the trajectory in Cartesian coordinates. Instead of timesteps, the method takes small negative α -steps from the original trajectory α_0 . At launch, the values of α , u , and \dot{s} are α_0 , u_0 , and V_0 , respectively. After α is decremented during an α -step, the updated values for u and \dot{s} are analytically obtained from equations 28 and 34, respectively. The exact trajectory pathlength increment associated with the α -step is analytically obtained as

$$ds = s - s^- = \frac{\ln(u/u^-)}{2B} , \quad (45)$$

where the “minus” superscript denotes values at the prior α -step. Directional components of this increment are used to update the Cartesian (x, y) coordinates from their initial values of $(0, H)$.

$$x = x^- + ds \cdot \cos \bar{\alpha} \quad (46)$$

$$y = y^- + ds \cdot \sin \bar{\alpha} , \quad (47)$$

where $\bar{\alpha} = (\alpha + \alpha^-)/2$. The time associated with α is obtained from ds and \dot{s} as follows:

$$t = t^- + ds/\dot{\bar{s}} , \quad (48)$$

where $\dot{\bar{s}} = (\dot{s} + \dot{s}^-)/2$. In this simple fashion, with successive α -steps, the time history of the trajectory may be obtained in Cartesian coordinates. A FORTRAN listing that implements this algorithm is given in table 1.

The results of this algorithm are demonstrated in figures 2–4. The simulation was for the trajectory of a 50 mm-long copper ($\rho_p = 8900 \text{ kg/m}^3$) projectile with a drag coefficient of 1.0, launched from an initial altitude of $H = 1 \text{ m}$ at a velocity of 2000 m/s and a launch angle of 25° . For these initial conditions, the value for the parameter B is 0.00145 m^{-1} . In these figures, a symbol is plotted for every 30 m of pathlength traveled. Recall that only x , y , and t are numerically integrated quantities. All other plotted values (including s , \dot{s} , $\dot{\alpha}$, and $d\alpha/ds$) are analytically defined in closed form. Of course, the same result could have been achieved through a conventional discretization and integration of the governing equations, equations 5 and 6. However, the advantage of the algorithm given in table 1 is computational speed and algorithmic simplicity.

Table 1. FORTRAN code listing

```

c      TRAJECTORY MODEL, WITH NUMERICAL INTEGRATION FOR CARTESIAN QUANTITIES
c
      implicit none
      integer n
      double precision B, V0, g, a, u, a0, H, da, C, u0, PI, af, ds,
&      x, y, t, uget, uf, sdot, s, dsprint, sdotf, adot
      data g, da, n, dsprint /9.806, -0.001, 1, 30./
      PARAMETER (PI = 3.1415926)

      print *, 'Enter B, Vo, alpha0, H: '
      read (*,*) B, V0, a0, H
      write(7, '(B, V0, a0, H: ', 1p4e11.4, /)') B, V0, a0, H
      write (7, '(V      alpha      s      x'',
&      '      y      t      da/dt''')
      a0 = a0 * PI/180.
      da = da * PI/180.

      u0 = g / (B * V0**2 * (cos(a0))**2)
      C = -uget(a0, -u0)
      PRINT *, 'u0, C: ', u0, C

c      INITIALIZE
      a = a0
      x = 0.
      y = H
      s = 0.
      sdot = V0
      t = 0.
      u = uget(a, C)
      adot = -sqrt(B*g*u)*(cos(a))**2
      write (7, '(7f10.3)') sdot, a * 180./PI, s, x, y, t, adot

c      ALPHA-STEP LOOP:
      do while (y .ge. 0.)

c          SAVE PRIOR ALPHA-STEP QUANTITIES; THEN STEP ALPHA
          uf = u
          sdotf = sdot
          a = a + da

c          GET CURRENT ALPHA-STEP QUANTITIES ANALYTICALLY
          u = uget(a, C)
          s = log(u/u0) / (2.*B)
          sdot = sqrt(g/(B*u)) / cos(a)
          ds = log(u/uf) / (2.*B)
          adot = -sqrt(B*g*u)*(cos(a))**2

c          HERE ARE THE INTEGRATED QUANTITIES
          x = x + ds * cos(a - da/2.)
          y = y + ds * sin(a - da/2.)
          t = t + 2.*ds/(sdot + sdotf)

c          CHECK IF TIME TO PRINT
          if (s .ge. float(n)*dsprint) then
              write (7, '(7f10.3)') sdot, a * 180./PI, s, x, y, t, adot
              n = n + 1
          end if
          if (abs(a) .le. -da/2.)
&      write (7, '(7f10.3)') sdot, a * 180./PI, s, x, y, t, adot
      end do
      write (7, '(7f10.3)') sdot, a * 180./PI, s, x, y, t, adot

      stop
      end
c*****
      double precision function uget(a, C)
      implicit none
      double precision a, C

      uget = C - tan(a)/cos(a) - log(tan(a) + 1./cos(a))
      return
      end

```

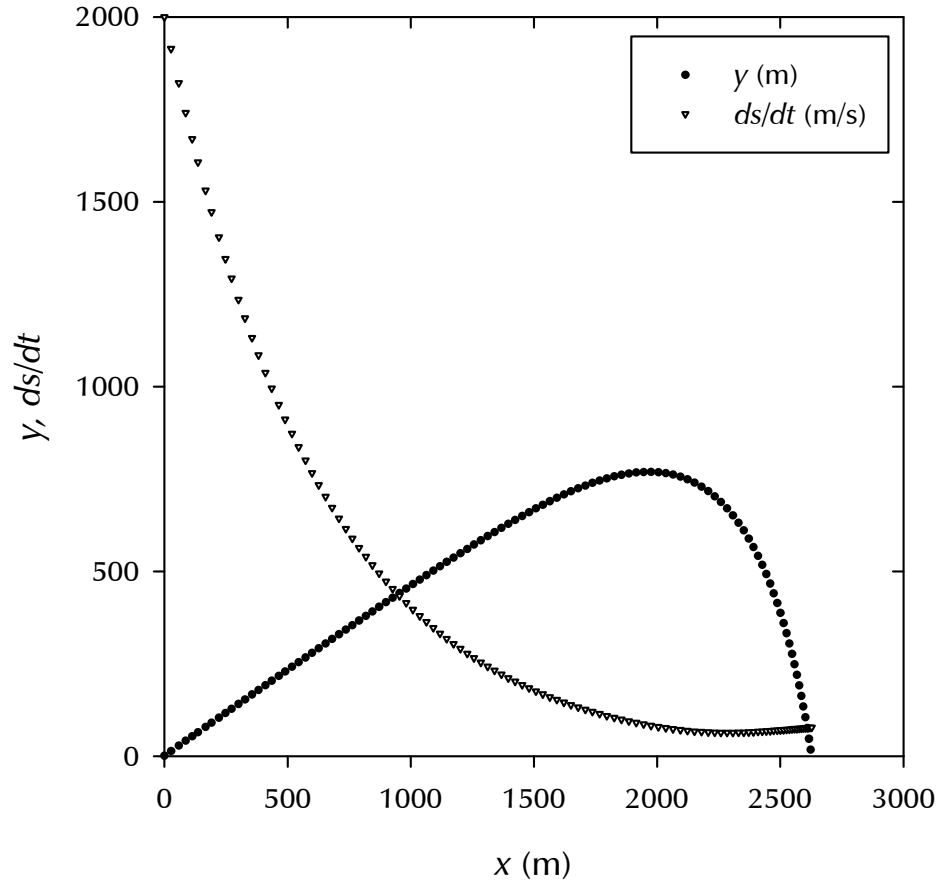


Figure 2. Trajectory (y) and velocity (ds/dt) for 50 mm-long copper ($\rho_p = 8900$ kg/m³) projectile with $C_d = 1.0$ ($B = 0.00145/\text{m}$) launched at 2000 m/s at an angle of $\alpha_0 = 25^\circ$ from an initial altitude of $H = 1$ m.

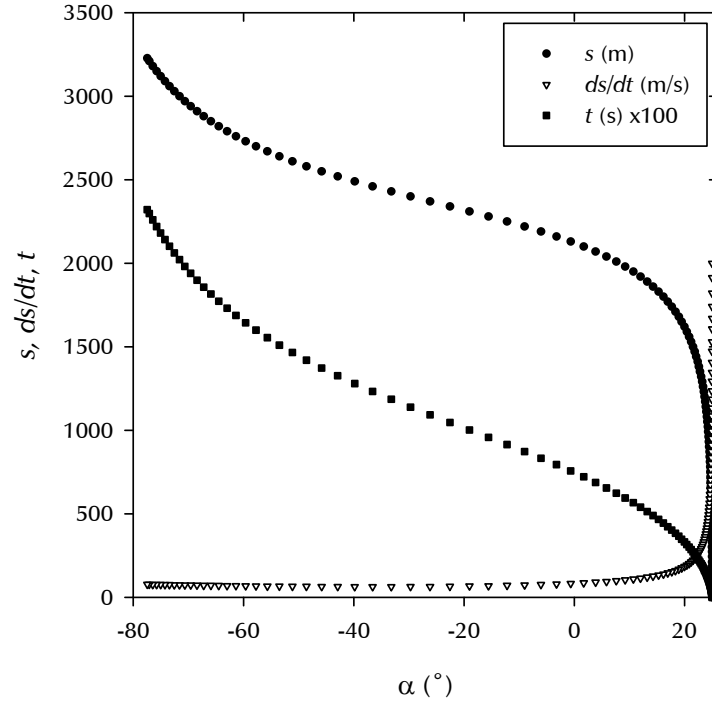


Figure 3. Pathlength (s), velocity (ds/dt), and flight time (t) as a function of trajectory angle (α).

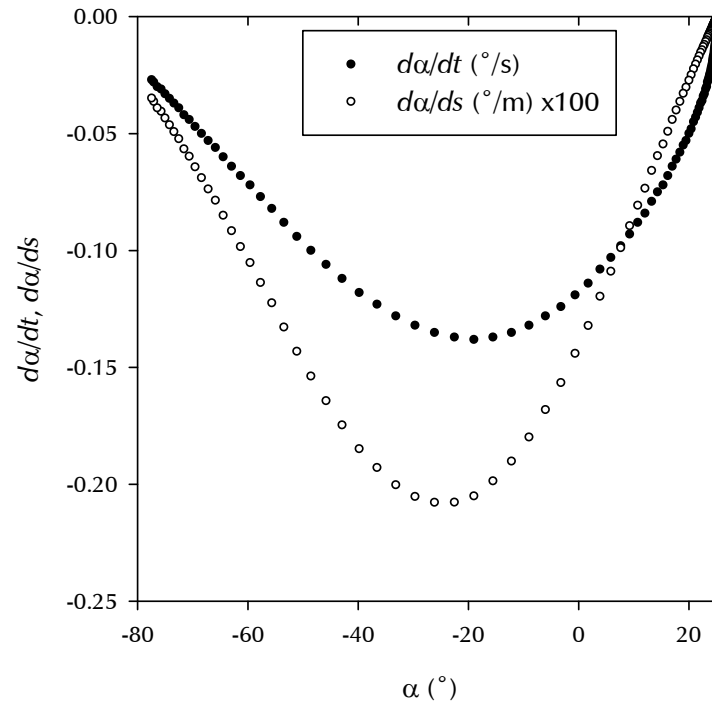


Figure 4. $\dot{\alpha}$ and $d\alpha/ds$ as a function of trajectory angle (α).

11. Special Case Solutions and Approximations

11.1 Approximate Cartesian Solution for Moderate Angle-of-attack Trajectories

While the *exact* trajectory solution has been presented in curvilinear coordinates (s, α) , it was made clear in section 9 that a corresponding analytical solution was not achieved in Cartesian coordinates (x, y) . Nonetheless, an excellent approximation can be derived, which is valid for trajectories through moderate angles of attack.

Let us separate the equations 29, 35, and 36 as follows:

$$dt = -\frac{1}{\sqrt{Bg}} \frac{\sec^2 \alpha}{\sqrt{u}} d\alpha \quad , \quad (49)$$

$$dx = \sqrt{\frac{g}{B}} \frac{dt}{\sqrt{u}} = -\frac{1}{B} \frac{\sec^2 \alpha}{u} d\alpha \quad , \quad (50)$$

and

$$dy = \tan \alpha \, dx = -\frac{1}{B} \frac{\tan \alpha \sec^2 \alpha}{u} d\alpha \quad . \quad (51)$$

While we have been unable to solve these integrals when u is accurately defined by equation 28, it is possible to develop an approximate solution by arbitrarily redefining an approximation to u (call it \hat{u}) that is both integrable in the context of equations 49–51 as well as approximately equal to equation 28 over a substantial range of the functional domain.

While there are many non-logarithmic functions that can be employed to very accurately approximate equation 28, their substitution into equations 49–51 must result in analytically integrable functions. Thus, the choices are quite limited, and the function we propose is

$$\hat{u} = \hat{C} - 2 \tan \alpha \quad . \quad (52)$$

There are two facets to this approximation to equation 28. One is the use of the constant \hat{C} as opposed to C . The other is the use of $2 \tan \alpha$ in place of $\tan \alpha \sec \alpha + \ln(\tan \alpha + \sec \alpha)$. As to \hat{C} , its specification, in order to rigorously satisfy the initial $t = 0$ condition, should be

$$\hat{C}(\text{nominal}) = u_0 + 2 \tan \alpha_0 = \frac{g \sec^2 \alpha_0}{BV_0^2} + 2 \tan \alpha_0 \quad . \quad (53)$$

However, since this development is part of an approximate solution, we are willing to relax rigor to achieve a better fit, as shown later.

For the second facet of the approximation, we see in figure 5 that the approximation given by $2 \tan \alpha$ is quite good up to $\pm 20^\circ$, and maybe acceptably good to a range of $\pm 40^\circ$. This range of applicability would cover quite a span of useful trajectories.

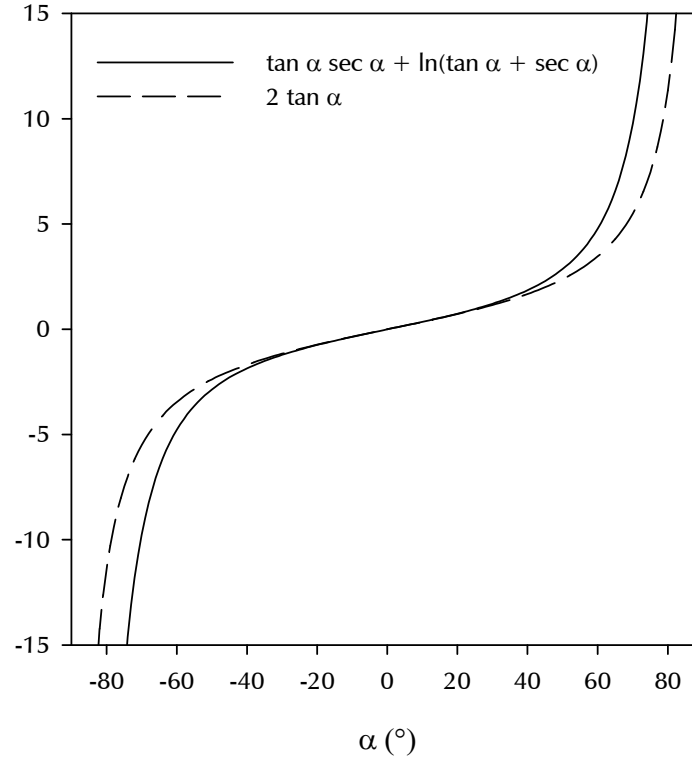


Figure 5. A comparison of $\tan \alpha \sec \alpha + \ln(\tan \alpha + \sec \alpha)$ to the approximation given by $2 \tan \alpha$.

Turning to equations 49–51, and employing the approximation to u given by equation 52, one may use the substitution $w = \tan \alpha$ to reexpress these governing equations as

$$dt = -\frac{1}{\sqrt{Bg}} \frac{dw}{\sqrt{\hat{C} - 2w}} \quad , \quad (54)$$

$$dx = -\frac{1}{B} \frac{dw}{\hat{C} - 2w} \quad , \quad (55)$$

and

$$dy = -\frac{1}{B} \frac{w dw}{\hat{C} - 2w} \quad . \quad (56)$$

These equations may be integrated directly to give the following:

$$t = \frac{1}{\sqrt{Bg}} \left(\sqrt{\hat{C} - 2w} - \sqrt{\hat{C} - 2w_0} \right) , \quad (57)$$

$$x = \frac{1}{2B} \ln \left(\frac{\hat{C} - 2w}{\hat{C} - 2w_0} \right) , \quad (58)$$

and

$$y - H = \frac{w - w_0}{2B} + \frac{\hat{C}}{4B} \ln \left(\frac{\hat{C} - 2w}{\hat{C} - 2w_0} \right) , \quad (59)$$

where w and w_0 are, respectively, $\tan \alpha$ and $\tan \alpha_0$; and H is the altitude of the launch point.

The equations for x and y may be alternately expressed, eliminating w , as

$$x = \frac{1}{B} \ln \left(1 + \frac{\sqrt{Bg} t}{\sqrt{\hat{C} - 2w_0}} \right) , \quad (60)$$

$$y = \frac{\hat{C}x}{2} - \frac{gt^2}{4} - \sqrt{\frac{g}{B}} \left(\frac{\hat{C}}{2} - w_0 \right) t + H . \quad (61)$$

We note that these alternate representations mimic the functional dependencies derived in an earlier shallow-trajectory model (5), though with different constants.

These approximate solutions were compared against the integrated trajectory of equations 46–47. The same trajectory problem was solved as presented in section 10, except for varying the initial trajectory angle, α_0 . On the basis of those results, the value of \hat{C} constant was refined from that given in equation 53 to a value of

$$\hat{C} = u_0(1 + 2.5 \tan^2 \alpha_0) + 2 \tan \alpha_0 , \quad (62)$$

in an effort to extend the applicability of the fit to larger angles of attack. The effect of modifying \hat{C} from its nominal value is to introduce a less accurate value of $\dot{\alpha}$ at $t = 0$, with the goal of improving the late-time trajectory approximation.[†]

With the approximations developed in equations 57–59 and the fit to \hat{C} given by equation 62, the trajectories are compared in figures 6–7. We see that, indeed, the approximation is excellent for initial trajectories at or below 20°, with trajectory range errors well below 1%, and altitude errors below 1.5%. The flight duration approximation was in error by under 4%, as well. As the

[†]Equation 62 was refined for this particular test case. A more general form, which tries to account for variabilities in B and V_0 , in addition to α_0 , is given by $\hat{C} = u_0 \{ 1 + 9/8 (V_0/V_{00})^3 / (1 + (V_0/V_{00})^3) [5.906 + 1.2 \log_{10}(B/B_0)] \tan^2 \alpha_0 \} + 2 \tan \alpha_0$, where $B_0 = 1 \text{ m}^{-1}$ and $V_{00} = 1000 \text{ m/s}$.

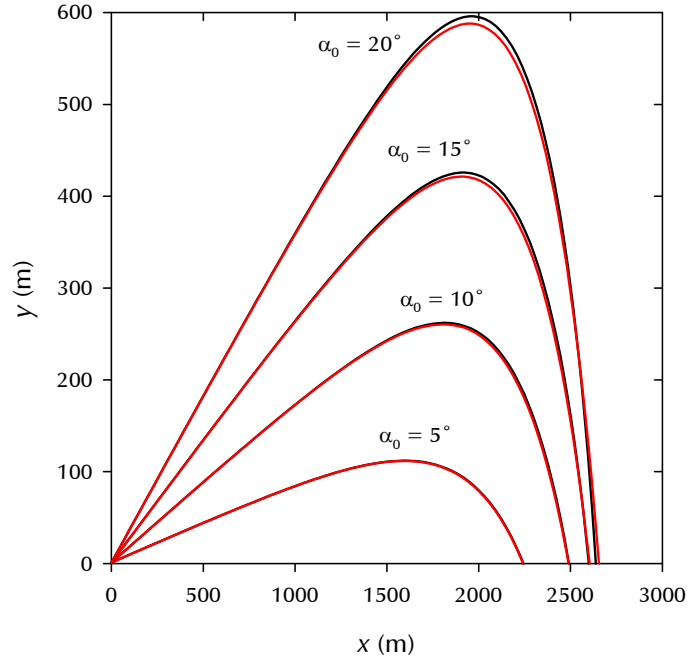


Figure 6. A comparison of numerically integrated (black) and approximated (red) trajectories for initial trajectory angles below 20° .

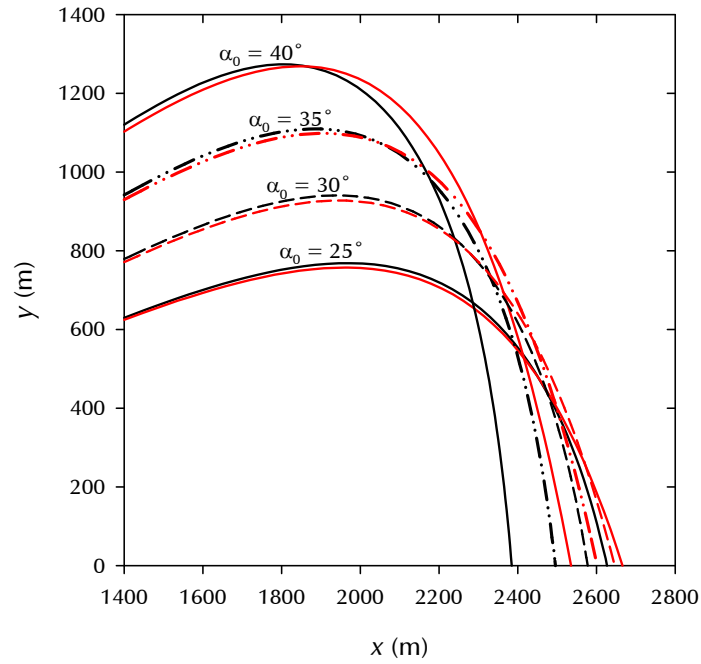


Figure 7. A comparison of numerically integrated (black) and approximated (red) trajectories for initial trajectory angles between 25° and 40° .

launch angle is increased beyond 20° , the approximation is less accurate at predicting total range, even as the approximation of maximum altitude remains of good quality.

But even so, at a 30° launch angle, the integrated maximum altitude is 941 m, whereas the approximated maximum altitude is 928 m, a 1.4% difference. The maximum horizontal range of that condition is integrated as 2578 m, and approximated as 2646 m, a mere 2.6% difference. The duration of the flight is 26.1 s when integrated, compared with 24.5 s when approximated, a 6.2% difference.

One notes that the approximation loses its greatest accuracy during the terminal phase of the trajectory. This can be explained through an examination of the original approximation found in figure 5. While α_0 starts out in a reasonable part of the fit, during the trajectory, α is monotonically decreasing. After the maximal altitude is reached at $\alpha = 0$, the value of α proceeds rapidly into the negative domain and, in the terminal phase of the trajectory, is reaching values in the vicinity of -80° , where the approximation offered by $2 \tan \alpha$ is particularly poor. However, even with these drawbacks at higher angles of attack, the results of the current Cartesian approximation (given by equations 57–59) were confirmed as more accurate than the shallow-angle trajectory approximation given in reference 5.

11.2 Maximum Pathlength from Launch to Apogee

While it is true that the *exact* trajectory solution was not expressed in Cartesian coordinates, one may nonetheless employ the curvilinear solution to glean interesting facets of the trajectory. For example, the apogee is the point in the trajectory of maximum altitude (where $\alpha = 0$). Since the value of u equals C at the apogee (equation 28), it immediately follows from equation 35 that the velocity at the apogee is $\sqrt{g/BC}$.

Whereas such details may be obtained through direct algebraic substitution, more complex information may also be derived from the solution. For example, the analytical solution may be employed to determine the launch angle needed to maximum the pathlength from launch point to apogee, as we demonstrate here.

The pathlength traversed, from launch to apogee, call it s_{ap} , is obtained from substituting equations 31 and 32 into equation 40:

$$s_{ap} = \frac{\ln(C/u_0)}{2B} = \frac{1}{2B} \ln \left[1 + \frac{BV_0^2}{g} \left(\frac{\tan \alpha_0}{\sec \alpha_0} + \frac{1}{\sec^2 \alpha_0} \ln(\tan \alpha_0 + \sec \alpha_0) \right) \right] . \quad (63)$$

To find the launch angle α_0 that maximizes s_{ap} , one merely need take $ds_{ap}/d\alpha_0$ and set the result

to zero. That process leads to the result that the maximum apogee pathlength is obtained for that value of α_0 , which satisfies the following relationship:

$$\ln(\tan \alpha_0 + \sec \alpha_0) = \csc \alpha_0 \quad [\text{for } \max(s_{ap})] \quad . \quad (64)$$

This relationship is satisfied when $\alpha_0 = 56.4656 \dots^\circ$, and is a very surprising relationship. It indicates that, regardless of the drag coefficient embodied in B , the initial launch velocity V_0 , and the gravitational constant g , the launch angle that maximizes the apogee pathlength is *always* 56.5° ! Indeed, through equation 63, the pathlength itself depends upon B , V_0 , and g , but the launch angle to maximize that apogee pathlength does not. This result has been computationally verified for trajectories under the influence of aerodynamic drag and analytically verified for drag-free (parabolic) trajectories.

11.3 Terminal Trajectory

When a trajectory is in its terminal stages, given enough altitude, it will approach the terminal velocity, which is given by $\sqrt{g/B}$. An examination of equation 34 for the projectile velocity, \dot{s} , reveals that, in the terminal phase, $\sqrt{u} \rightarrow \sec \alpha$, in order for the velocity to approach its terminal value.

Therefore, if we substitute $\sec \alpha$ for the appearance of \sqrt{u} , thereby forcing the projectile velocity to remain fixed at the terminal velocity, we should be able to learn something of the terminal trajectory. Let us use the t subscript to define variables at the onset of the terminal phase.

First, consider equation 29, which defines $\dot{\alpha}$. Once \sqrt{u} is replaced with $\sec \alpha$, the equation may be separated to solve for dt and then integrated:

$$\int_{t_t}^t dt = -\frac{1}{\sqrt{Bg}} \int_{\alpha_t}^{\alpha} \sec \alpha \, d\alpha \quad , \quad (65)$$

resulting in

$$t - t_t = \frac{1}{\sqrt{Bg}} \ln \left(\frac{\sec \alpha_t + \tan \alpha_t}{\sec \alpha + \tan \alpha} \right) \quad . \quad (66)$$

Recall that, in the terminal phase, α will be negative, and tending towards -90° .

Turning to the x coordinate of the trajectory, the same approximation may be made to equation 35 to obtain

$$\int_{x_t}^x dx = -\frac{1}{B} \int_{\alpha_t}^{\alpha} d\alpha \quad , \quad (67)$$

leading to

$$x - x_t = -\frac{1}{B}(\alpha - \alpha_t) \quad . \quad (68)$$

Similarly for y ,

$$\int_{y_t}^y dy = -\frac{1}{B} \int_{\alpha_t}^{\alpha} \tan \alpha \, d\alpha \quad , \quad (69)$$

leading to

$$y - y_t = \frac{1}{B} \ln \left(\frac{\sec \alpha_t}{\sec \alpha} \right) \quad . \quad (70)$$

These results bear some similarity to the 1920 report by Wilson (1) on bomb trajectories, in which the y trajectory is approximated in various ways, the sixth such approximation being expressed largely in terms of a $-\ln(\sec x)$ term.

To see how this function of terminal trajectory compares to the exact solution, we provide figure 8, which zooms in on the terminal phase of the trajectory described in figure 2. Superimposed on the graph are three instances of the approximated terminal trajectory implicitly given by equations 68 and 70. In these three terminal trajectories, the starting point associated with (x_t, y_t) corresponds, respectively, to α_t values of 0° , -30° , and -60° . Obviously, the closer α_t is taken to -90° , the more accurate the estimate of the terminal trajectory will be.

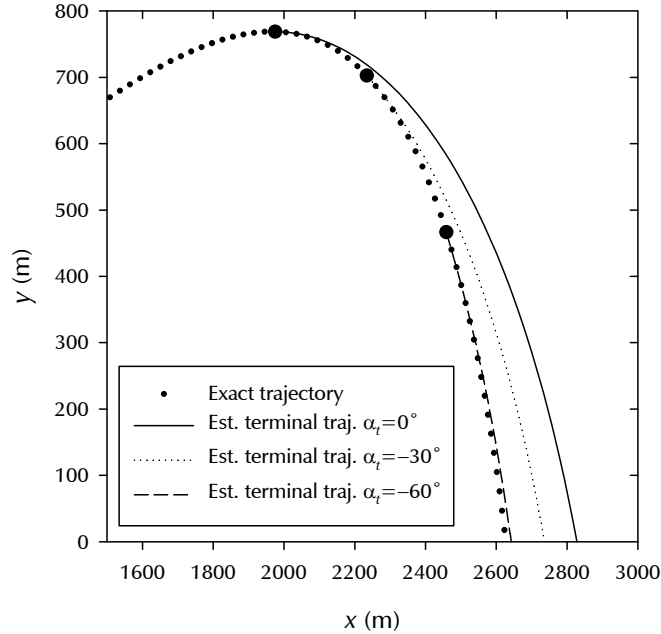


Figure 8. Estimated terminal trajectories from three starting points on the actual trajectory, corresponding to α_t equal to 0° , -30° , and -60° , respectively.

12. Conclusions

The solution to the problem of low-altitude ballistic trajectory, under the influence of a uniform gravitational field and aerodynamic drag, has been presented here. By “ballistic,” we are limiting the analysis to a projectile that possesses neither propulsion nor lift. The solution was achieved through a transformation of the governing equations into a curvilinear coordinate system. The solution provides for the pathlength of the trajectory in terms of the trajectory angle. Also available from the solution are the velocities along the pathlength; the vertical and horizontal velocity components; and the time rate of change of the trajectory angle. In all cases, these variables are expressed in terms of the current trajectory angle.

Unfortunately, there are useful functions of interest that are not analytically accessible from the solution. These include the Cartesian (x, y) coordinates of the trajectory and the time required to reach various stages of the trajectory. Also, the solution cannot be mathematically inverted. As a result, the trajectory angle must remain the independent variable of the problem, and cannot be analytically expressed in terms of other quantities along the trajectory.

To increase the utility of the solution, when a Cartesian solution is essential, an integration algorithm was presented, which makes use of the exact solution, in order to expedite the calculation of the Cartesian time history of the trajectory. In the algorithm presented, the discretized integration variable is not time, as would traditionally be the case when employing a brute-force approach to the problem, but rather the trajectory angle. The algorithm was demonstrated on a sample problem, and the results were graphically presented.

Several special-case solutions were offered, including an analytical approximation to the Cartesian solution, quite accurate up to moderate angle-of-attack trajectories (less than 20° , approximately), and reasonably accurate beyond that (*e.g.*, up to 30°). Further, an unexpected analytical result was developed, which shows that the trajectory that maximizes the apogee-pathlength (*i.e.*, pathlength from launch to apogee) is 56.5° , regardless of launch velocity, drag coefficient (including drag-free parabolic trajectories), and gravitational constant.

13. References

1. Wilson, E. B. *Bomb Trajectories*; NACA Report 79; National Advisory Committee for Aeronautics, 1920.
2. Hou, S. Measurement of the Location of Impact Point in Bombing Systems. In *Proceedings of the First International Conference on Pervasive Computing, Signal Processing and Applications (IEEE)*, Harbin Heilongjiang, China, 17–19 September 2010.
3. Wikipedia. “Trajectory of a Projectile.”
http://en.wikipedia.org/wiki/Trajectory_of_a_projectile. (accessed October, 2011).
4. NASA. “Flight Equations with Drag.”
<http://www.grc.nasa.gov/WWW/k-12/airplane/flteqs.html>. (accessed October, 2011).
5. Walters, W. P.; Segletes, S. B. *Distance Traveled by a Hypervelocity Projectile in Air*; ARL-TR-5612; U.S. Army Research Laboratory: Aberdeen Proving Ground, Maryland, July 2011.
6. Moss, G. M. Range Danger Area Assessment for Shaped Charge Warheads. In *Proc. 14th International Symposium on Ballistics*, Quebec City, Canada, 26–29 September 1993.

<u>NO. OF COPIES</u>	<u>ORGANIZATION</u>
1 (PDF ONLY)	DEFENSE TECHNICAL INFORMATION CTR DTIC OCA 8725 JOHN J KINGMAN RD STE 0944 FORT BELVOIR VA 22060-6218
1	DIRECTOR US ARMY RESEARCH LAB IMNE ALC HRR 2800 POWDER MILL RD ADELPHI MD 20783-1197
1	DIRECTOR US ARMY RESEARCH LAB RDRL CIO LL 2800 POWDER MILL RD ADELPHI MD 20783-1197
1	DIRECTOR US ARMY RESEARCH LAB RDRL CIO MT 2800 POWDER MILL RD ADELPHI MD 20783-1197
1	DIRECTOR US ARMY RESEARCH LAB RDRL D 2800 POWDER MILL RD ADELPHI MD 20783-1197

<u>NO. OF COPIES</u>	<u>ORGANIZATION</u>
1	AIR FORCE ARMAMENT LAB AFATL DLJR D LAMBERT EGLIN AFB FL 32542-6810
3	COMMANDER US ARMY ARDEC RDAR MEE W E BAKER A DANIELS R FONG B3022 PICATINNY ARSENAL NJ 07806-5000
2	COMMANDER US ARMY AVN & MISSILE CMD AMSAM RD PS WF S CORNELIUS S HOWARD REDSTONE ARSENAL AL 35898-5247
2	DARPA W SNOWDEN S WAX 3701 N FAIRFAX DR ARLINGTON VA 22203-1714
1	SANDIA NATIONAL LABORATORIES S SCHUMACHER PO BOX 5800 ALBUQUERQUE NM 87185-MS0836
9	LLNL R E TIPTON L-095 D BAUM L-163 M MURPHY L-099 T MCABEE L-095 G POMYKAL L-072 J E REAUGH L-282 R M KUKLO L-099 G SIMONSON L-099 R BARKER L-020 PO BOX 808 LIVERMORE CA 94550

<u>NO. OF COPIES</u>	<u>ORGANIZATION</u>
5	LOS ALAMOS NATL LABORATORY L HULL MS A133 C WINGATE MS D413 C RAGAN MS D449 E J CHAPYAK MS F664 J BOLSTAD MS G787 PO BOX 1663 LOS ALAMOS NM 87545
3	SOUTHWEST RESEARCH INST C ANDERSON S A MULLIN J WALKER PO DRAWER 28510 SAN ANTONIO TX 78228-0510
3	DE TECHNOLOGIES R CICCARELLI W FLIS W CLARK 100 QUEENS DR KING OF PRUSSIA PA 19406
1	DREXEL UNIVERSITY MEM DEPT B FAROUK 32ND & CHESTNUT ST PHILADELPHIA PA 19104
1	VIRGINIA POLYTECHNIC INSTITUTE COLLEGE OF ENGINEERING DEPT ENGN G SCI & MECHANICS R C BATRA BLACKSBURG VA 24061-0219
1	KERLEY PUBLISHING SERVICES G I KERLEY PO BOX 709 APPOMATOX VA 24522-0709
1	TEXTRON DEFNS SYS C MILLER 201 LOWELL ST WILMINGTON MA 01887-4113
1	LOCKHEED MARTIN ELECT & MIS G W BROOKS 5600 SAND LAKE RD MP 544 ORLANDO FL 32819-8907

<u>NO. OF COPIES</u>	<u>ORGANIZATION</u>
2	GD OTS D BOEKA N OUYE 2950 MERCED ST STE 131 SAN LEANDRO CA 94577
1	JAMS PROJECT OFFICE ATTN: SFAE-MSLS-JAMS-SYS-O C ALLEN 5250 MARTIN RD REDSTONE ARSENAL AL 35898
1	HALLIBURTON ENERGY SVCS JET RESEARCH CTR D LEIDEL PO BOX 327 ALVARADO TX 76009-9775
1	GEN CORP AEROJET D PILLASCH B57 D3700 1100 W HOLLYVALE ST AZUSA CA 91702
1	INTRNTL RSRCH ASSOC D ORPHAL 4450 BLACK AVE PLEASANTON CA 94566-6105

<u>NO. OF COPIES</u>	<u>ORGANIZATION</u>
	<u>ABERDEEN PROVING GROUND</u>
69	DIR USARL RDRL SL P TANENBAUM RDRL SLB R BOWEN RDRL SLB D R GROTE L MOSS J POLESNE RDRL SLB E M PERRY C BARKER D FORDYCE P HORTON D HOWLE D LYNCH M MAHAFFEY R SAUCIER RDRL SLB G P MERGLER RDRL SLB S R BOWERS M OMALLEY RDRL SLB W L ROACH J ABELL W MERMAGEN RDRL WM P PLOSTINS RDRL WMS T ROSENBERGER RDRL WML M ZOLTOSKI RDRL WML C K MCNESBY RDRL WML H T EHLERS T FARRAND E KENNEDY L MAGNESS C MEYER B SORENSEN R SUMMERS RDRL WMM B G GAZONAS RDRL WMP P BAKER S SCHOENFELD RDRL WMP B

<u>NO. OF</u> <u>COPIES</u>	<u>ORGANIZATION</u>
	C HOPPEL
	S R BILYK
	D CASEM
	M GREENFIELD
	C WILLIAMS
	RDRL WMP C
	T BJERKE
	J BARB
	N BRUCHEY
	T DIGLIANI
	R MUDD
	S SEGLETES (5 COPIES)
	W WALTERS (5 COPIES)
	RDRL WMP D
	J RUNYEON
	R FREY
	D KLEPONIS
	H W MEYER
	B SCOTT
	K STOFFEL
	RDRL WMP E
	M BURKINS
	W A GOOCH
	E HORWATH
	B LOVE
	RDRL WMP F
	N GNIAZDOWSKI
	E FIORAVANTE
	RDRL WMP G
	N ELDREDGE
	W BUKOWSKI
	R EHLERS
	S KUKUCK

<u>NO. OF COPIES</u>	<u>ORGANIZATION</u>
1	A. LUKYANOV ABINGDON TECHNOLOGY CENTRE SCHLUMBERGER ABINGDON OX14 1UJ UNITED KINGDOM
1	E ROMENSKI SOBOLEV INSTITUTE OF MATHEMATICS SB RAS NOVOSIBIRSK 630090 RUSSIA
1	S SCHMAUDER INST MATERIALS TESTING, MATERIALS SCIENCE AND STRENGTH OF MATERIALS UNIVERSITY OF STUTTGART PFAFFENWALDRING 32 D-70569 STUTTGART GERMANY
1	V PETROVA DEPARTMENT OF MATHEMATICS VORONEZH STATE UNIVERSITY UNIVERSITY SQ 1 VORONEZH 394006 RUSSIA
1	J C F MILLETT DEPARTMENT OF HYDRODYNAMICS AWE ALDERMASTON READING RG7 4 PR UNITED KINGDOM
1	ST. PETERSBURG STATE TECHNICAL UNIVERSITY FACULTY OF PHYS AND MECHANICS DEPT OF THEORETICAL MECHANICS ATTN: A M KRIVTSOV POLITECHNICHESKAYA STREET 29 195251 ST-PETERSBURG RUSSIA
2	RUSSIAN FEDERAL NUCLEAR CENTER - VNIIEF L F GUDARENKO R F TRUNIN MIRA AVE., 37 SAROV 607190 RUSSIA

<u>NO. OF COPIES</u>	<u>ORGANIZATION</u>
1	ROYAL MILITARY ACADEMY G DYCKMANS RENAISSANCELAAN 30 1000 BRUSSELS BELGIUM
1	NORDMETALL GMBH L W MEYER EIBENBERG EINSIEDLER STR 18 H D-09235 BURKHARDTSDORF GERMANY
2	TU CHEMNITZ L W MEYER (x2) FAKULTAET FUER MASCHINENBAU LEHRSTUHL WERKSTOFFE DES MASCHINENBAUS D-09107 CHEMNITZ GERMANY
4	INSTITUTE OF CHEMICAL PHYSICS RUSSIAN ACADEMY OF SCIENCES G I KANEL A M MOLODETS S V RAZORENOV A V UTKIN 142432 CHERNOGOLOVKA MOSCOW REGION RUSSIA
3	INSTITUTE OF MECH ENGINEERING PROBLEMS V BULATOV D INDEITSEV Y MESCHERYAKOV BOLSHOY, 61, V.O. ST PETERSBURG 199178 RUSSIA
1	SAMARA STATE AEROSPACE UNIV L G LUKASHEV SAMARA RUSSIA
1	TOMSK STATE UNIVERSITY A G GERASIMOV 5-TH ARMY STREET, 29-61 TOMSK 634024 RUSSIA

<u>NO. OF COPIES</u>	<u>ORGANIZATION</u>
1	DEFENCE SCIENCE & TECH LAB PHYSICAL SCIENCES DEPT D POPE PORTON DOWN SALISBURY SP4 0JQ UNITED KINGDOM